

## Research Article

# Spatially defined oxygen gradients and vascular endothelial growth factor expression in an engineered 3D cell model

U. Cheema<sup>a,\*</sup>, R. A. Brown<sup>a</sup>, B. Alp<sup>a</sup> and A. J. MacRobert<sup>b</sup>

<sup>a</sup> University College London, Tissue Repair and Engineering Centre, Institute of Orthopaedics and Musculoskeletal Sciences, Stanmore Campus, London HA7 4LP (UK), Fax: +44 208 954 8560, e-mail: u.cheema@ucl.ac.uk

<sup>b</sup> National Medical Laser Centre, Royal Free and University College Medical School, London (UK)

Received 3 August 2007; received after revision 24 October 2007; accepted 29 October 2007

Online First 13 November 2007

**Abstract.** Tissue hypoxia results in rapid angiogenesis *in vivo*, triggered by angiogenic proteins, including vascular endothelial growth factor (VEGF). Current views of tissue viability are founded on whether ‘deeper-lying’ cells receive sufficient nutrients and oxygen for normal activity and ultimately survival. For intact tissues, levels of such essential nutrients are governed by micro-vascular perfusion. However, there have been few effective quantitatively defined 3D models, which enable testing of the interplay or interdependence of matrix and cell density, and path diffusion on oxygen consumption *in vitro*. As a result,

concepts on cell vulnerability to low oxygen levels, together with the nature of cellular responses are ill defined. The present study has adapted a novel, optical fibre-based system for *in situ*, real-time oxygen monitoring within three-dimensionally-spiralled cellular collagen constructs, which were then unfurled to enable quantitative, spatial measurements of VEGF production in different parts of the same construct exposed to different oxygen levels. A VEGF response was elicited by cells exposed to low oxygen levels (20 mmHg), primarily within the construct core.

**Keywords.** Oxygen monitoring, cellular hypoxia, 3D culture, tissue construct, VEGF, plastic compression, collagen, cell death, tissue engineering.

## Introduction

Only by growth of cells in 3D is it possible to mimic and investigate the role of spatial factors on changing cell morphology, biochemistry and gene expression [1, 2]. This has been made possible by removing cells from their native tissue (complex and ill-defined) and growing them in a simplified, controlled matrix such as native collagen hydro-gels [3–5]. However, there is a common assertion, but poorly defined concern, that

the core of such engineered 3D tissue models, both *in vitro* and *in vivo*, will suffer rapid cell death through oxygen and nutrient depletion in the core. The effects of limiting perfusion can be established by relating oxygen or nutrient gradients (over time and space) to: (i) scaffold material properties, (ii) cell density, (iii) cell activity and (iv) diffusion distances. Our aim is to establish a 3D tissue-like model suitable for quantitative measurement of the relation between available levels of O<sub>2</sub> and cell responses in 3D. Clearly it is critical that controlling scaffold factors such as cell density and matrix permeability are: (a) definable (b) controllable and (c) comparable to native tissues.

\* Corresponding author.

While a great deal is understood about oxygen requirements of cells in monolayers, it is currently difficult to convincingly model such behaviour in 3D. As a result, extrapolation from 2D culture or 3D native tissue is frequently oversimplified. The practical importance of this knowledge cannot be over emphasised in the progression towards tissue-engineered implants and reduction of animal usage for testing, as both are seriously impaired by limitations of available 3D model systems.

Mammalian tissues operate in oxygen tensions ranging from 2% to 10% oxygen, or partial pressures ( $pO_2$ ) of 15–75 mmHg, which represents the natural environment for their survival [6]. This range is distinct from what is termed ‘pathological’ hypoxia (<1%  $O_2$  or <8 mmHg), which is considered to be low oxygen tension resulting in the compromised metabolism of cells in tissues *in vivo* [6]. Studies have been conducted to measure the fluctuating levels of oxygen at the cell surface in 2D tissue culture [7, 8]. In early studies, the oxygen tension measured directly over a cell layer fluctuated between 20 and 80 mmHg, suggesting that entire cell populations modulate their respiration in synchrony, as a result of an environmental feedback dependent on depletion (exhaustion) and renewal (diffusion) of essential nutrients [7]. This is crucial in understanding basic cellular requirements and consumption of oxygen, and these data have allowed some level of correlation with cell behaviour, at least in cell sheets. When cells are grown in 2D as a monolayer, many of the imperatives of the 3D environment in which cells normally reside are lost, and some crucial structural dynamics altered. Using cells in a native, tissue-like extracellular matrix, it becomes possible to test the detailed responses and key factors controlling all behaviour in response to oxygen depletion. For this it is also essential to establish the precise  $O_2$  consumption dynamics in distinct zones of the construct (potentially tens of micrometers apart), in relation to local cell responses over prolonged periods. In this respect, conventional electrode technology for  $pO_2$  measurements suffers from a number of disadvantages, in particular local, artefactual  $pO_2$  depletion resulting from consumption by the probe itself. The present study has adapted a novel optical fibre-based system for *in situ*, real-time  $pO_2$  monitoring within collagen constructs. The key features of the fibre-optic probes are that they exhibit a stable calibrated response together with negligible local oxygen consumption.

It is known that high oxygen tensions induce oxidative stress (23%, >170 mmHg) due to mitochondrial respiration, whereas low oxygen tension (<1.1 kPa or <8 mmHg) induce cells to undergo energetic stress [9]. Therefore, a balance in intracellular oxygen levels,

which is relatively low, is crucial to avoid oxidative stress and protect bioenergetic efficiency [9]. However, in 3D culture, as in native tissues, cells at different locations must experience different levels of perfusion, within a working range. Clearly it is important to understand the limits of these ranges for a given cell type and their likely responses where environments fall outside that range. The present study has focused on identifying the level and time period to elicit low level oxygen responses by testing the hypothesis that a key fibroblast response is likely to be the production of signals to promote angiogenesis.

Although there is currently much emphasis on the use of polymer scaffolds for tissue modelling [10, 11], we have chosen to use native type I collagen nano-fibrillar scaffolds, where the percentage of collagen is increased, and so mechanical integrity is also enhanced, through a process of plastic compression [12]. Such 3D matrices have highly biomimetic composition and micro-architecture and, indeed, mechanical and diffusive properties, which can be controlled to the levels needed for precise modelling. As collagen type I is the predominant extracellular matrix component in most mammalian tissues (along with other minor components including glycoproteins, glycosaminoglycans and proteoglycans), it remains a good material to use for studies of cellular behaviour in 3D. The hypothesis was that fibroblasts would not die rapidly even deep within a dense collagen matrix, but will undergo progressive changes in their gene expression, particularly of angiogenic signalling molecules. The aim was to quantitatively assess, by actual measurement of  $O_2$  tension zones and correlate this with actual levels of  $O_2$  in defined 3D constructs. Using defined cell densities in defined 3D constructs over a 10-day period, we have been able to monitor real-time oxygen levels with high sensitivity and precision at the core and surface of 3D constructs. The present study demonstrates that this model is effective in identifying key control mechanisms of growth factor regulation (*i.e.*, vascular endothelial growth factor, VEGF) by cells in 3D. This represents the first time such detailed correlations have been possible under such biomimetic, 3D-controlled conditions.

## Methods

**Cell culture and expansion.** Human dermal neonatal fibroblasts were explanted from neonatal foreskins (obtained freshly from the operating theatre, with full ethical approval, following surgery for circumcision), as previously described [13]. Cells were maintained in Dulbecco’s modified Eagles medium (DMEM, Gibco,

Paisley, UK), supplemented with 10% FCS (First Link, West Midlands, UK), 2 mM glutamine and penicillin/streptomycin (1000 U/ml; 100 µg/ml, Gibco Chemicals). For removal of cells from monolayer culture, flasks containing cells were washed with 0.1 M PBS, and incubated with trypsin (0.5% in 5 mM EDTA) for 5 min at 37 °C.

**3D plastic compressed collagen gel culture.** Once detached, cells were counted and embedded in 3D collagen type I gels. Collagen gels were set in a mould ( $2.2 \times 3.3 \times 1 \text{ cm}^3$ ). For collagen gel preparation, 0.5 ml  $10 \times$  Eagles MEM solution (Gibco) was added to 4 ml rat-tail type I collagen (First Link) in 0.1 M acetic acid, protein concentration 2.035 mg/ml, neutralized with 5 M NaOH, using the indicator colour changes from yellow to cirrus pink [14]. This gel preparation was added to the cell suspension. Following setting and incubation, gels were routinely compacted by a combination of compression and blotting using layers of mesh and paper sheets [12]. Briefly, 165-µm-thick stainless steel mesh and a layer of nylon mesh were placed on a double layer of absorbent paper. The collagen gel was placed on the nylon mesh, covered with a second nylon mesh, and loaded with a 120-g flat metal block (steel) for 5 min at room temperature, giving a flat collagen sheet (50–60 µm thick) protected between two nylon meshes. These dense sheets of collagen were then rolled to produce a tight spirally wound rod, 2.3 mm in diameter and 21 mm long. Cell densities were increased by the plastic compression in direct proportion to the volume reduction of gel and final cell density was calculated as: initial cell density  $\times$  fold volume change. Hence for a typical initial gel volume of 5 ml, the percentage of collagen was 0.2%, which increased to 11% following compression (measured by dry/wet weight ratio), which corresponds to a 58-fold increase. The cell density would be expected to change by the same degree from a total of 100 000 cells/ml (or 0.5 million cells/construct) to a final density of 5.8 million cells/ml; 200 000 cells/ml (or 1 million cells/construct) to 11.6 million cells/ml; 400 000 cells/ml (or 2 million cells/construct) to 23.2 million cells/ml [15].

**Oxygen monitoring.** Fibre-optic oxygen probes (Oxford Optronix, Oxford, UK) were inserted into the centre of the 3D spiral constructs and positioned halfway along its axis (Fig. 1a). The constructs were then sealed at the end using cyanoacrylate glue. Hence, a diffusion length of  $> 1$  mm was studied and refers mainly to lateral diffusion, as the ends of the construct were sealed. The tip of the sensor probe (280 µm diameter) incorporates an oxygen-sensitive luminescent probe within an oxygen-permeable

matrix. The luminescence is quenched in the presence of molecular oxygen so that the luminescence emission lifetime becomes longer at lower oxygen concentrations in the surrounding medium. The calibration of the probe, which is accurate to 0.7 mmHg, essentially relies on the correlation of the luminescence lifetime (rather than intensity) *versus* the oxygen concentration [16]. This method results in an exceptionally stable calibrated response so that each probe may be used up to 6 days at the slowest sampling rate. Therefore, for monitoring of constructs for longer than 6 days, the expiring probes were removed and new probes inserted on day 5 (see below). After each experiment, the probe reading was checked in the external medium to confirm that there was no drift in the response. The fibre-optic probes were used in conjunction with an OxyLab pO<sub>2</sub> E<sup>TM</sup> system coupled to an A/D converter (12 bit) and the results were recorded on an IBM PC computer using Labview. Results are presented as partial pressure values, *i.e.*, pO<sub>2</sub> in mmHg (*e.g.*, 7.6 mmHg corresponds to 1% oxygen). The sampling rate was varied according to the experiment performed, yielding an overall response time of  $< 10$  s (for de-oxygenation measurements, Fig. 1b, c) and up to  $\sim 30$  s for the long-term studies as shown in Figure 2. For studies of the rate of oxygen diffusion through the construct, we transferred the construct containing the probe into an anoxic solution of 3% sodium sulphite at 37 °C. Rates of de-oxygenation and re-oxygenation were estimated using the quasi-linear portions of the traces, as shown in Figure 1. Samples were kept and monitored in 7.5% CO<sub>2</sub>-enriched incubators. At the end of each experiment the construct was removed and the ambient O<sub>2</sub> tension of the media tested, which remained at approximately 140 mmHg.

**Cell viability.** Cell viability was assessed using Live/Dead Viability/Cytotoxicity Kit (Molecular Probes, L-3224) based on the simultaneous determination of live and dead cells with calcein AM and ethidium homodimer (EthD-1), respectively, for qualitative analysis. Quantitative analyses were carried out with Live/Dead Reduced Biohazard Viability/Cytotoxicity Kit (Molecular Probes, L-7013) according to the manufacturer's protocol. SYTO<sup>®</sup> 10, a green fluorescent nucleic acid stain and Dead Red (ethidium homodimer-2) were used, and, after capturing images, live/dead nuclei were counted to ascertain percentage viability. Viability of cells in each construct was performed independently from the oxygen measurements. Representative areas for O<sub>2</sub> determination were chosen in two regions (core and surface) of plastic compressed constructs and were visualized

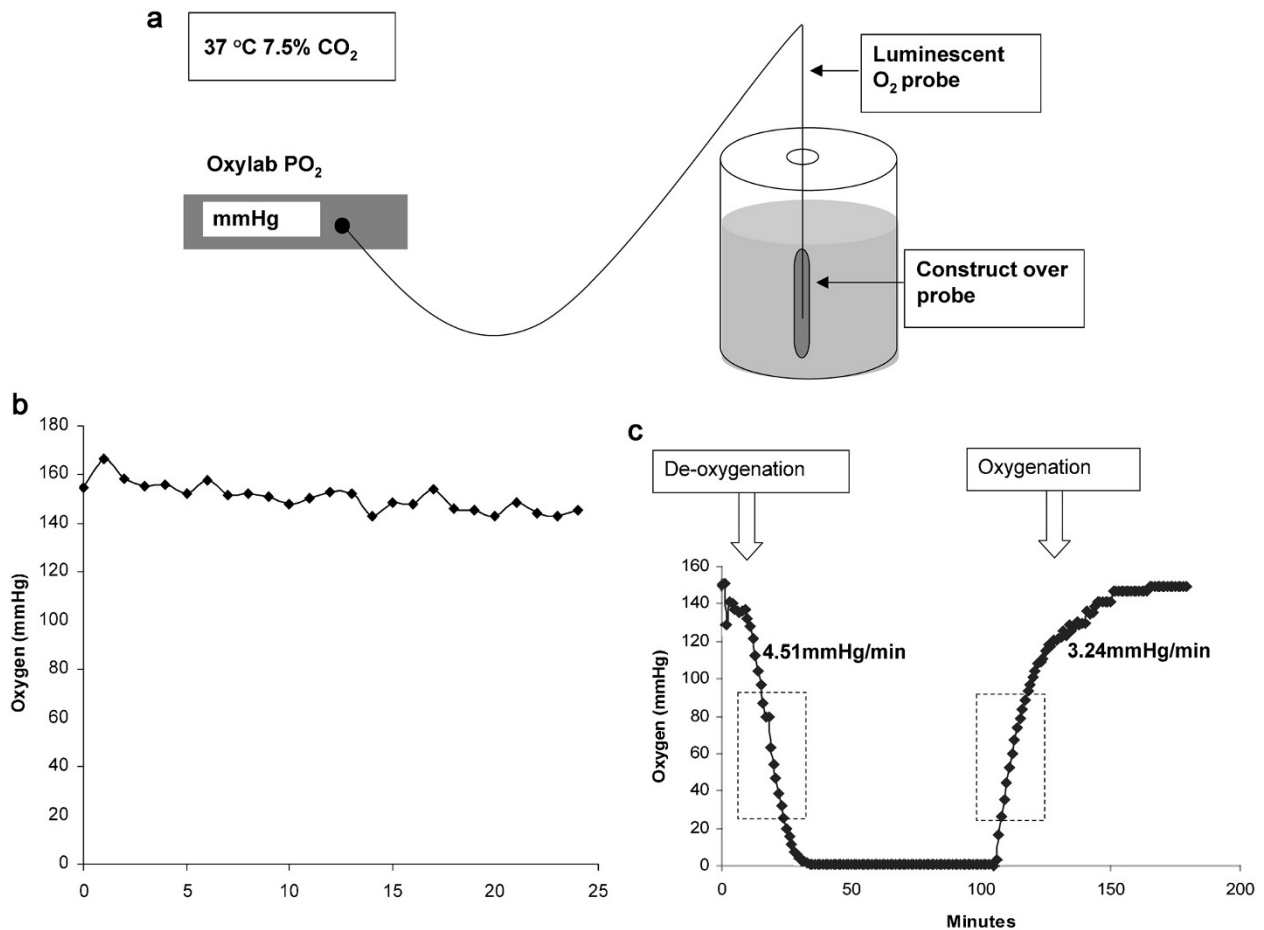


**Figure 1.** (a) Schematic of the experimental set up, with O<sub>2</sub> probe in the centre of a spiralled plastic compression construct. Constructs were cultured in 50 ml media. (b) Graph showing O<sub>2</sub> levels in the centre of acellular plastic compression constructs. (c) Graph showing the de-oxygenation of an acellular plastic compression construct with sodium sulphite, followed by oxygenation in DMEM media (values of  $4.5 \pm 0.5$  and  $3.2 \pm 0.5$  mmHg/min). The gradients (corresponding to de-oxygenation and re-oxygenation rates) were estimated using the approximately linear portions of the traces.

with confocal microscopy (Bio-Rad Radiance 2100, Carl Zeiss Ltd, Hertfordshire, UK).

**Quantitative PCR analysis of VEGF mRNA.** RNA extraction from experimental constructs was performed independently from the oxygen measurements. RNA was extracted either from the whole construct, or from specific regions of the spiral construct (core, mid and surface). These regions were isolated after culture by unrolling the spirals and cutting into the three different regions corresponding to core, mid and surface. Total cellular RNA was isolated from the cellular 3D plastic compressed constructs using the Qiagen RNeasy method (Qiagen, UK). Constructs were first flash-frozen in liquid nitrogen, and 500  $\mu$ l lysis buffer containing 2-mercaptoethanol was added to each sample and left to dissolve at room temperature for 40 min (Qiagen, UK). The resultant solution was then aspirated using a 21-G needle and from then on the commercial assay

protocol was followed (Qiagen, UK). RNA was eluted in RNase-free water, and the concentration determined by spectrophotometry at 260 and 280 nm (Genequant, Pharmacia Biotech, NJ, USA).

First strand cDNA synthesis was performed using Amplitaq reverse transcriptase (Applied Biosystems, Roche). Total RNA (0.5  $\mu$ g RNA) was diluted in 38.85  $\mu$ l water. A further 9.15  $\mu$ l Mastermix was added to each tube (dNTP, RNase inhibitor, MgCl<sub>2</sub>, Oligo DT Random primers; Applied Biosystems, Roche), and heated at 70 °C for 10 min; 2  $\mu$ l reverse transcriptase was then added to each tube and tubes were incubated at 40 °C for 1.5 h, followed by heating at 90 °C for 2 min to denature any remaining enzyme.

**Real-time quantitative PCR for VEGF.** Relative quantitative PCR was performed using Applied Biosystems 7300 Real-time PCR system (CA, USA), with the Taqman universal PCR Master Mix (Applied Biosystems). cDNA, 9  $\mu$ l/reaction, was mixed with

1  $\mu\text{L}$  of the required gene probe (VEGF, Applied Biosystems assay ID: Hs00900057\_m1 or GAPDH, Applied Biosystems assay ID: Hs99999905\_m1) and 10  $\mu\text{L}$  Mastermix (Applied Biosystems) in a 96-well plate for cycling and analysis in the Applied Biosystems 7300 Real-time PCR machine (total 20- $\mu\text{L}$  reaction volume). The primer sequences are not disclosed and kept confidential by Applied Biosystems (Roche). Each primer set is calibrated to work optimally in the 7300 Real-time PCR machine. The combined thermal cycling and amplification-specific software enabled detection of the PCR products as cycle-by-cycle accumulation in a single-tube reaction. Values for each sample were normalised to the corresponding GAPDH result, which did not change significantly in any sample tested. Relative quantification was performed by expressing each sample/GAPDH ratio relative to a calibrator. This calibrator was set as 2 million cells per construct at 1 day. This calibrator was run along each run tested and compared. By doing this, any small changes from run to run could be accounted for, as we were relying on relative quantification. This calibrator was measured in each PCR run (with no significant variation) and was always set to unity, and the sample change expressed as fold increase or decrease relative to this. In the case of cell density, culture period and region experiments, this was set as 2 million cells/construct at 24 h. Therefore, all relative quantification of gene expression changes were set relative to this.

## Results

The 3D monitoring set-up is shown schematically in Figure 1a. Validation and calibration studies on constructs without cells (Fig. 1b) showed a steady baseline level of  $\text{O}_2$  tension in the core of cell-free constructs, with negligible consumption of oxygen over 24 h (not significantly different from the external medium), consistent with minimal  $\text{O}_2$  consumption of the probe. Cell-independent depletion and recovery of core  $\text{O}_2$  levels was demonstrated (Fig. 1c) by addition and then removal and washout of a 3% solution of sodium sulphite to sequester  $\text{O}_2$  from the system. The oxygen levels were observed to fall progressively over several minutes, reaching zero after approximately 30 min. Note that the time response of the probes itself was set to  $<10$  s. Recovery back to air-saturated  $p\text{O}_2$  levels was measured by transferring the construct still containing the probe back into an air-saturated solution, which occurred at an approximate rate of  $3.2 \pm 0.5$  mmHg/min. Comparable rapid rates of re-equilibration were seen using  $\text{N}_2$  saturation of medium instead of the sodium sulphite reagent.

Cellular constructs exhibited time-dependent oxygen depletion in their core, where the probe was positioned, over a period of 24 h (Fig. 2a). Oxygen levels fell rapidly towards approximately steady-state or plateau values, which varied according to the cell density. Cell consumption, therefore, appeared to be the only factor influencing oxygen levels in the

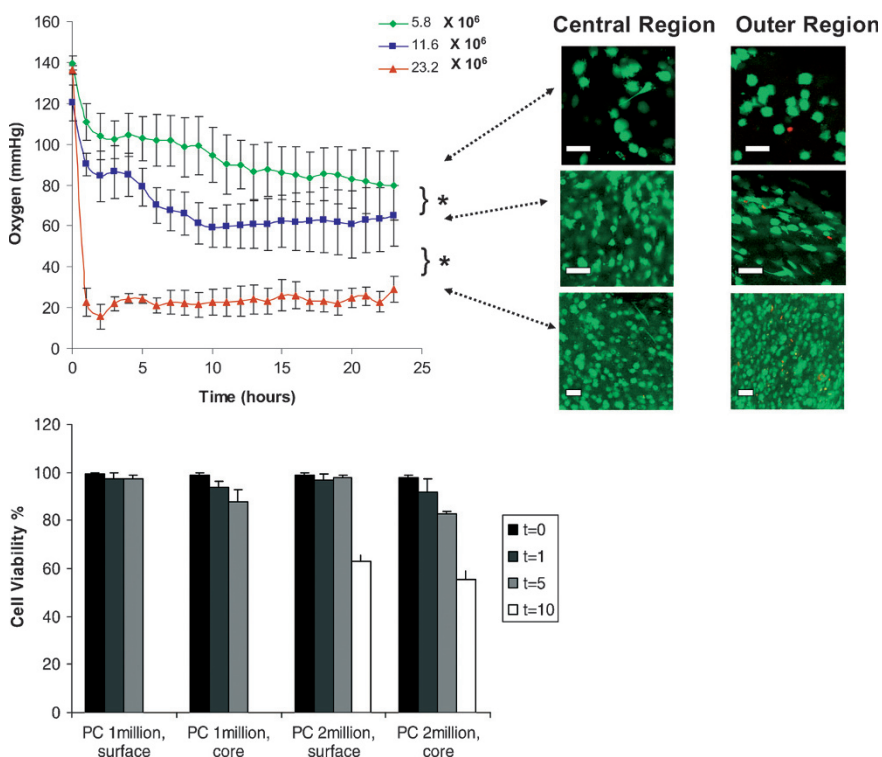


**Figure 2.** (a) Oxygen levels in the centre of cell-seeded plastic compression constructs with supporting confocal images of the central and outer region of the construct. Different cell densities were measured,  $5.8 \times 10^6 - 23.2 \times 10^6$  cells/ml, magnification bar 50  $\mu\text{m}$  ( $0.5 \times 10^6 - 2 \times 10^6$  cells/construct), \*  $p < 0.0001$ . Average of  $n = 3$  for each data set is presented here. Time 'zero' is taken as the time point when the probe was positioned in the construct. (b) Cell viability measured after 0 h, and 1, 5 and 10 days in static cultures. \* **Fig. 2 (b)** had been omitted in the Online First version of this article and was included in an erratum (DOI 10.1007/s00018-007-7000-7).

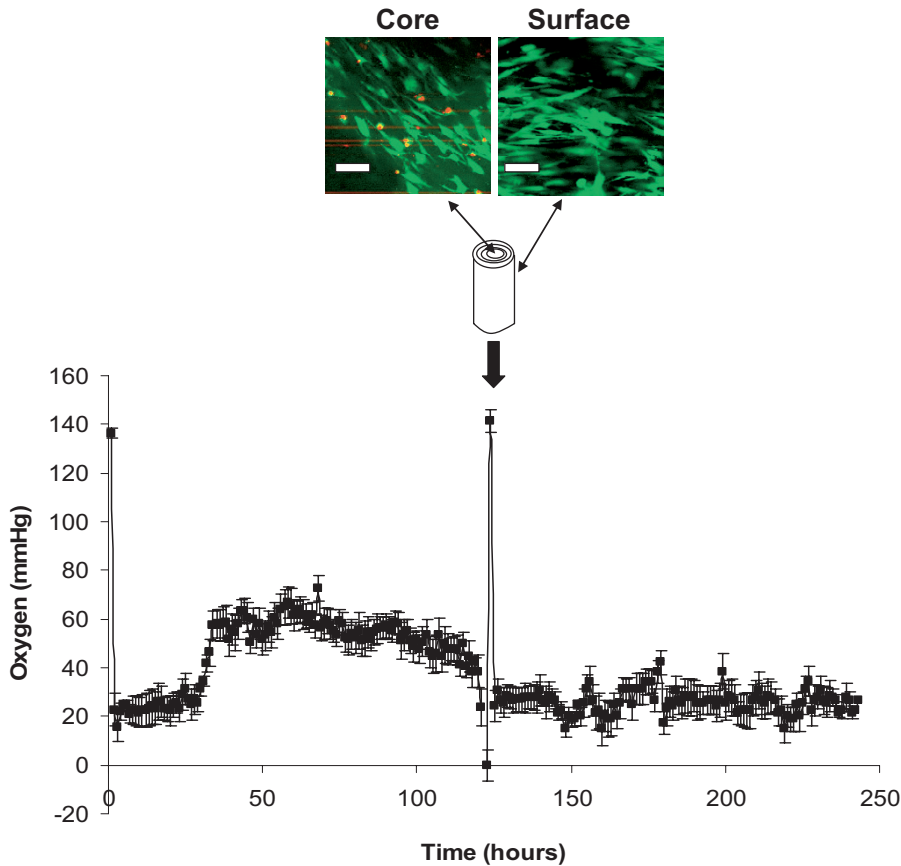


**Figure 3.** Oxygen levels in the centre of a cell-seeded construct,  $2 \times 10^6$  cells in a construct ( $23.2 \times 10^6$  cells/ml), over a 10-day period, with supporting cell viability on day 5 (Fig. 2b) from the centre and surface of the construct (note: it was technically necessary to carry out the 10-day experiment in two parts: days 0–5 and 6–10, with the re-start at day 5, therefore a composite of two 5-day measurements in sequence is shown). Graph represents a mean of  $n = 3$ . Magnification bar 100  $\mu$ m for micrographs.

construct. Cell density was the key determining factor in the degree of oxygen depletion response, with the lower core  $pO_2$  correlating with the higher cell density, which ranged from 0, 5.8, 11.6 to 23.2 million cells/ml. In this case, the plateau  $O_2$  tensions declined significantly ( $p < 0.001$ ) with each increase in cell density. The oxygen level in the centre of constructs seeded with 0.5 million cells (final density of 5.8 million cells/ml) was around 80 mmHg after 24 h, compared to a construct seeded with 2 million cells (final cell density of 23.2 million cells/ml), where the level was  $\sim 25$  mmHg. Exposure of cells to low levels of oxygen in the core had no effect on cell viability over this 24-h period. Cells in the construct core had over 95 % viability after exposure to both 80 mmHg and 25 mmHg (Fig. 2b). Hence exposure of cells to oxygen tensions as low as 25 mmHg did not increase cell death up to 5 days. At day 10, up to 55 % cell death was observed in the core, compared to 40 % at the surface. In such a 3D model, the diffusion of critical higher molecular weight nutrients may also be a limiting factor for cell survival. Glucose diffusion coefficients have previously been established and this is not found to be limiting for cells in the same 3D model [17].

Figure 3a shows the core  $O_2$  profile, over a 10-day period, of a construct seeded at an initial cell density

of 2 million cells (23.2 million cells/ml). Importantly, after the initial 24-h fall to a first equilibrium level of  $\sim 25$  mmHg, core oxygen tension increased to a second elevated steady state of around 60 mmHg. This is likely to be a result of changes in cell consumption rather than changes in material properties (Fig. 3a). Over the 10-day period, there were no major changes in cell number through proliferation (unpublished observation). After 5 days, core cell viability was still 80 %, and close to 100 % at the surface. Hence, between the 30- and 36-h culture periods, the stabilised core  $O_2$  tension rose by 35 mmHg ( $>$  twofold increase), to approximately 60 mmHg. This occurred over a 6-h period, consistent with a change in fibroblast metabolism and  $O_2$  utilisation. This level was approximately maintained over the following 24 h and then fell gradually back to  $\sim 20$  mmHg over the following 72 h.

Levels of VEGF mRNA expression were measured in constructs at the three cell densities studied and in the 23.2 million cells/ml construct over 10 days of culture (Fig. 4). At the 24-h stage, the three cell densities gave relative VEGF gene expression levels with no significant difference, shown here relative to the highest cell density (Fig. 4a).

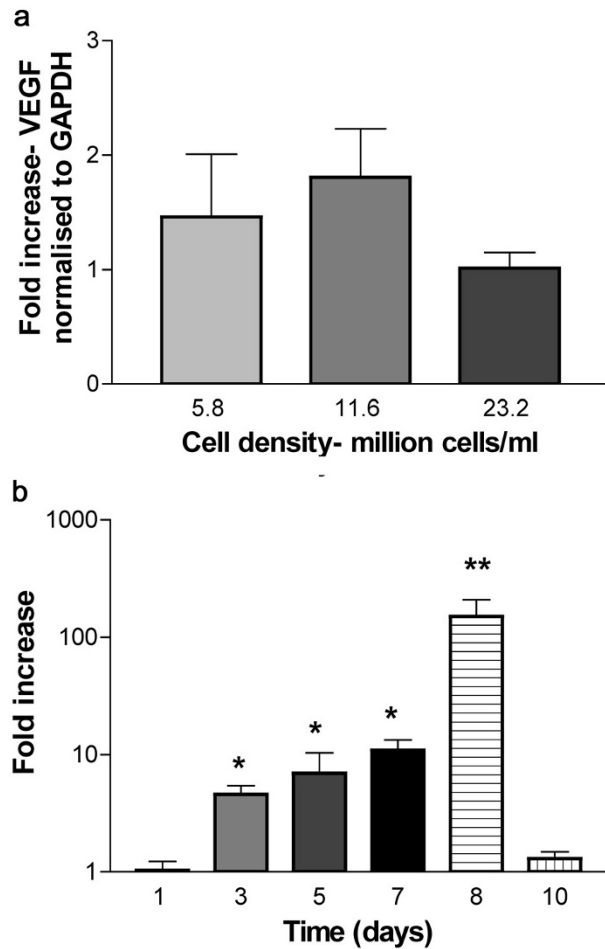


**Figure 4.** Fold increase in the expression of VEGF mRNA in 3D constructs. (a) VEGF levels in constructs of varying cell density at 24 h. No significant difference was found in VEGF levels between the different cell densities. (b) The level of VEGF in constructs containing 2 million cells/construct over a 10-day period (normalised to GAPDH, with day 1 as the set calibrator) shows a statistically significant increase measured on day 8, which then dropped by day 10 (\*\*  $p < 0.001$ , \*  $p < 0.05$ ).

Over the longer 10-day period, VEGF expression levels changed dramatically in the 23.2 million cells/ml constructs (Fig. 4b). Between days 1 and 3 (23.2 million cells/ml) there was a 5-fold increase in VEGF expression ( $p < 0.05$ ), followed by small incremental increases between days 3 and 7, reaching an 11-fold increase over day 1 levels ( $p < 0.05$ ). The greatest changes, however, were seen between days 7 and 8. Expression leapt by 140-fold, to a total of 151-fold greater than day 1. This was followed almost immediately by a complete collapse in expression (149-fold), such that by day 10 expression had returned back to day 1 levels. This pattern of an apparent temporal spike of growth factor expression would be characteristic of control systems based on a number of different molecular elements operating in sequence as might be expected for angiogenic stim-

ulation. Such a spike in VEGF expression would be expected where only one growth factor of a sequential cocktail was monitored, as in this system. This pattern of VEGF regulation over 10 days was not observed with the lower cell densities studied (data not shown). Zonal changes in VEGF expression, through the thickness of the spiral constructs (23.2 million cells/ml) and so along the gradient of  $O_2$  tension, were determined at the 8-day culture stage (core, mid and surface). Zonal changes were measured by unfurling the spiral construct after culturing (Fig. 5). It was assumed that cells in the core section of the gel, which was the zone sampled by the probe, had been exposed to  $O_2$  levels between 20 and 60 mmHg, in the mid section to between 60 and 100 mmHg, and in the outer section, which was in close proximity to the aerated medium, to between 100 and 140 mmHg over most of the culture period. Significantly higher levels of VEGF were found in the core region, where cells were exposed to the lowest levels of  $O_2$ . Figure 5 shows the gradient of VEGF expression at 8 day (23.2 million cells/ml) under these conditions (*i.e.*, the underlying zonal heterogeneity at day 8). Importantly cells in the surface region still expressed increased levels of message (4.7-fold increase over basal 1-day VEGF levels). In the mid and core regions this increased to 7.1- and 10.1-fold greater expression than 1-day levels, consistent with a direct relationship between  $O_2$  tension and VEGF gene expression. However, given high  $O_2$  tensions found in the surface zone, this suggests that cells were either extremely sensitive to very modest reductions in available  $O_2$  or, more plausibly, surface zone cells had responded to earlier stage cytokine or metabolic signals (not measured here) produced and diffusing out from the core cells. This suggests a system exists for amplifying the zone of increased VEGF expression.

## Discussion and conclusions

Current views of tissue viability and 3D cellular constructs are dominated by the ability of 'deep-lying' cells to receive sufficient nutrient and oxygen for normal activity and ultimately for survival. In intact tissues such factors are clearly controlled by the presence and rates of micro-vascular perfusion. In the absence of this process, in 3D culture, cells rely entirely on simple diffusion from the construct margins. However, there have been few, if any, effective quantitatively defined 3D models that enable testing of the interplay of matrix density and cell density on  $O_2$  depletion. As a result, concepts on cell vulnerability to low  $O_2$ , together with the rate, extent and nature of their responses (short of cell death) are

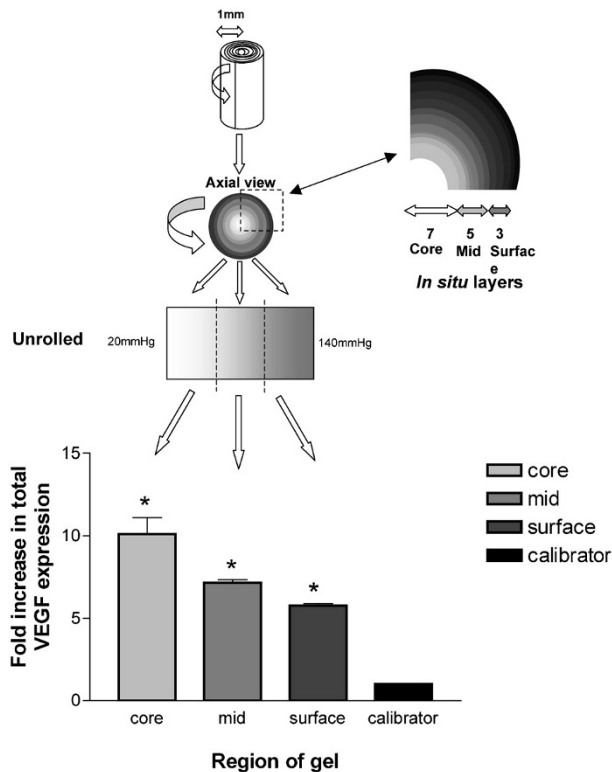


**Figure 5.** Spiral constructs seeded with  $2 \times 10^6$  cells were cultured for 8 days (peak in VEGF expression) and unrolled to study VEGF in three regions of the construct (because of spiralling these regions corresponded to three unequal thicknesses of the original construct core, mid and surface, approximately 7, 5 and 3 layers respectively). VEGF expression was normalised to GAPDH, with day 1 as the set calibrator, which was  $23.2 \times 10^6$  cells/ml at 24 h (the same calibrator for Fig. 4a and b). There were significantly higher levels of VEGF found in the centre of the gels ( $*p < 0.001$ ); however, this was not found to be directly proportional to the values obtained on day 8 in the time series, and certainly the core values are less than expected. This is likely to be the effect of using relative quantification, and the cumulative result previously obtained of the three regions.

simplistic. Importantly, many are based on tumour or other cell masses, with little or no extracellular matrix content. However, new technologies now make it possible to produce 3D cultured constructs with definable, near-native properties and to measure  $O_2$  precisely and locally. The present study has developed the first 3D-monitored model of connective tissue to define precisely which factors dominate and how they affect resident cell behaviour and survival. Using this model, the time-dependence of oxygen *versus* VEGF was studied over several days together with spatial measurements.

There are several key determining factors in this system, as there are *in vivo*, for the level and rate of attainment of minimum  $O_2$  tension at the core (furthest from perfusion point) of 3D constructs and tissues: (1) cell density, which is assumed to be a homogenous distribution, but can change zonally and

over time, (2) matrix density/permeability to the limiting diffusing component ( $O_2$  or other nutrient), and (3) cell type or cell activity (*i.e.*,  $O_2$  demand of the cells, which is dependent on aerobic/anaerobic and active/quiescent status; *e.g.*, chondrocyte, dermal fibroblast, myoblast). The plastic compression process for the 3D collagen constructs provides control of all these factors. The cell and matrix densities are both determined by the initial inoculum and initial collagen content (respectively) multiplied by the fold compression ( $\times 58$ ). The collagen matrix has a nano-fibrillar lattice of around 88% water, making it highly permeable to  $O_2$ .

The initial rate of consumption of  $O_2$  was non-linear over the first 10–30 min of the experiment, but thereafter was nearly constant (data not shown). In this system the rate of fall of  $O_2$  and the equilibrium consumption of  $O_2$  was entirely predictive, being dependent on cell density (Fig. 2a). Despite the relatively high matrix density and resultant  $O_2$  depletion at the centre of the constructs, cell viability was unaffected at 24 h and only slightly reduced ( $> 80\%$  of cells viable) after 5 days at the highest cell density (Fig. 3). To relate this to other work on cell responses to low levels of  $O_2$ , pathological hypoxia is conventionally set at  $< 1\%$  or 8 mmHg [6, 18]. Consequently,  $pO_2$  levels in the core of high cell density constructs here never fell below 18 mmHg, and so were not conventionally hypoxic (Fig. 3). This challenges the conventional impression that diffusion gradients  $> 1$  mm are frequently damaging to cells, but supports the idea that dense fibrillar collagen represents only a modest diffusion barrier (*i.e.*, highly permeable to small molecules). This high permeability to  $O_2$  is reasonable given the nano-fibrillar mesh structure of the matrix, with approximately 88% fluid phase. This was established here by the  $O_2$  re-equilibrium rate (1-mm shortest diffusion path) of  $4.5 \pm 0.5$  mmHg/min. Importantly, the greater reductions in core  $O_2$  tension were apparently cell number dependent, suggesting that it is not necessarily matrix diffusion path length that dominates cell response, but the number of overlying cell layers, each depleting  $O_2$ . This provides an insight into understanding why the core of cell-rich, matrix-poor structures (tumours, organs) are so much more vulnerable to core cell necrosis compared to connective tissues. The overall levels of VEGF measured in the different regions were significantly lower compared to the total day 8 reading. We postulate that this is due to slow processing of the constructs since they had to be unrolled carefully, during which time (up to 1 h) the values of VEGF may have dropped as cells in the entire construct became exposed to normoxia, including the core region during the final stage of unrolling.



Cells exposed to low oxygen tensions respond by significant increases in TGF- $\beta$ , platelet-derived growth factor (PDGF) and VEGF expression, and this would be expected in present 3D constructs cultures, which have 20 mmHg  $pO_2$  for considerable periods in the core [19–21]. It seems likely, therefore, that some exposure to low levels of oxygen is in fact complementary to tissue construct maturation, and will in fact be beneficial to cell survival. The influence of varying  $O_2$  tension on cellular proliferation and differentiation is crucial in understanding how physiological microenvironments can influence cellular behaviour, and there has been work to show that low levels of oxygen enhance proliferation of many cell types, including fibroblasts [22, 23].

Cell growth at reduced  $O_2$  tension does not necessarily result in cell death. When cultured at 2% oxygen (~ 15.2 mmHg), trophoblast cell proliferation is stimulated, whereas at 20% (152 mmHg), cells actually exit the cell cycle, and undergo increased differentiation [22]. Reduced  $O_2$  tensions measured in the current study (down to as low as 15 mmHg), were close to those used in the study by Ma et al. [22], and while direct extrapolation is dangerous here, due to differences in cell type and cell density, some parallels can be drawn. For instance, it does highlight the paradox of suggestions that 3D cell/matrix culture composites may undergo cell death in the centre due to oxygen depletion, in contrast to data indicating that reduced levels of  $O_2$  tension in tissue culture can enhance cell proliferation and indeed mimic many native cell environments. Precise and 3D-localised measurement of  $O_2$  tension is, therefore, critical in determining our understanding of any given 3D tissue model. It may, for example, be necessary to manipulate both high and low levels of oxygen locally to stimulate at different stages cell proliferation and cell differentiation for maturation of the model.

The first of three cell reactions to prolonged low  $O_2$  tension (> 24 h, high density) was an apparent shift to anaerobic metabolism, indicated by the relative increase in  $O_2$  tension after 23 h (Fig. 2). Although confirmation of this was beyond the scope of this study, such a shift to predominantly glycolytic metabolism seems the most reasonable explanation, given that changes in cell number or matrix permeability capable of explaining this rise in core  $O_2$  can be ruled out in this instance. Such a concerted shift in cell metabolism would not be surprising, although its trigger may well be specific to fibroblasts. It does, however, suggest that such cells do have low  $O_2$  responses, even above conventional pathological hypoxia and these this may trigger further downstream responses.

Most tissue repair and tissue engineering integration processes depend on rapid angiogenesis, triggered by

a number of angiogenic proteins, including VEGF. VEGF expression is induced by the transcription factor HIF-1 $\alpha$ , which possesses an oxygen-sensitive degradation domain [24, 25]. Large increases in VEGF mRNA levels were measured by day 8 in cell-dense constructs. One trigger for this up-regulation may be low levels of  $O_2$  or a resultant sustained period of glycolytic metabolism [26]. Confirmation that cell death was not significant here (> 80% cell viability at day 5) is important, since it indicates that the VEGF response was not dependent on dying cells. However, by day 10, a reduction in cell viability was measured and this have been the predominant reason VEGF levels dropped on day 10. Furthermore, it was possible to demonstrate that much (although not all) of the VEGF response was due to cells at the construct core, where levels were assumed to range between 20 and 60 mmHg compared to 100 and 140 mmHg at the construct surface. This was achievable because as the 3D spiral model could be unfurled, following the oxygen measurements, which then allowed us to quantitatively map out where VEGF production was up-regulated, with regards to the spatial position. The exposure of cells to  $O_2$  was dependent on the specific region they were located within the gel construct, which correspondingly influenced VEGF levels. Critically, the up-regulation of VEGF was not observed up to 24 h, when constructs were seeded with different cell densities (and therefore exposed to different  $O_2$  gradients within the constructs). The gradients varied from 82 to 140 mmHg (0.5 million), 66 to 140 mmHg (1 million), and 23 to 140 mmHg (2 million). This controlled *in vitro* system allowed the  $O_2$ -dependent VEGF regulation to be monitored carefully. As levels of  $O_2$  did not fall below 15 mmHg, and certainly not as low as 7.6 mmHg (1% oxygen), it cannot be said that the trigger for VEGF up-regulation is classical “pathological hypoxia”. The signalling of this low level of  $O_2$  (within physiological hypoxia range) to the cells to stimulate VEGF is therefore likely to be through initial up-regulation of its transcription factor, HIF-1 $\alpha$ .

In summary, we have established a basic model for the study of  $O_2$  consumption by human dermal fibroblasts in 3D collagen matrices. It was clearly evident that no adverse affect on cell viability was observed due to lower levels of oxygen exposure. In turn, the pattern of VEGF regulation has been determined under low  $pO_2$  but non-hypoxic conditions. A clear understanding of the differences between cell responses at the low end of the normal range, as opposed to true, damaging hypoxia is important, especially within the context of 3D tissue culture models, where local control of all growth factor production is central to spatial organisation. By combining our model, for instance, with

work on the changes in cell cycle regulation dependent on O<sub>2</sub> level, it may be possible to alter O<sub>2</sub> tensions in constructs to induce a shift away from cell proliferation and towards differentiation [22].

This study also raises the possibility of engineering naturally occurring angiogenic signals for induction of vascularisation in such 3D tissue engineered constructs post implantation. It is possible that if VEGF, along with other cell-manufactured angiogenic signals, were produced mainly in a 3D construct core, with lower levels produced by cells the closer they got to the surface, a gradient of these signals would induce vascularisation from the surface of a 3D construct towards the core, potentially inducing vascularisation from outside the construct in an *in vivo* scenario. For instance, by understanding when and where cells at defined densities and within a defined matrix will up-regulate VEGF production could be used to promote implant integration *in vivo*.

**Acknowledgements.** This work was supported by the Biotechnology and Biological Sciences Research Council, UK. We would like to thank Nicky Mordan for technical assistance with the confocal microscopy.

- 1 Weaver, V. M., Petersen, O. W., Wang, F., Larabell, C. A., Briand, P., Damsky, C. and Bissell, M. J. (1997) Reversion of the malignant phenotype of human breast cells in three-dimensional culture and *in vivo* by integrin blocking antibodies. *J. Cell Biol.* 137, 231–245.
- 2 Wang, F., Weaver, V. M., Petersen, O. W., Larabell, C. A., Dedhar, S., Briand, P., Lupa, R. and Bissell, M. J. (1998) Reciprocal interactions between beta1-integrin and epidermal growth factor receptor in three-dimensional basement membrane breast cultures: a different perspective in epithelial biology. *Proc. Natl. Acad. Sci. USA* 95, 14821–14826.
- 3 Weiss, P. (1959) Cellular dynamics. *Rev. Mod. Phys.* 31, 11–20.
- 4 Tomasek, J. J., Gabbiani, G., Hinz, B., Chaponnier, C. and Brown, R. A. (2002) Myofibroblasts and mechano-regulation of connective tissue remodelling. *Nat. Rev. Mol. Cell Biol.* 3, 349–363.
- 5 Grinnell, F. (2003) Fibroblast biology in three-dimensional collagen matrices. *Trends Cell Biol.* 13, 264–269.
- 6 Okazaki, K. M. and Maltepe, E. (2006) Oxygen, epigenetics and stem cell fate. *Regen. Med.* 1, 71–83.
- 7 Werrlein, R. J. and Glinos, A. D. (1974) Oxygen microenvironment and respiratory oscillations in cultured mammalian cells. *Nature* 251, 317–319.
- 8 Tokuda, Y., Crane, S., Yamaguchi, Y., Zhou, L. and Falanga, V. (2000) The levels and kinetics of oxygen tension detectable at the surface of human dermal fibroblast cultures. *J. Cell Physiol.* 182, 414–420.
- 9 Gnaiger, E., Mendez, G. and Hand, S. C. (2000) High phosphorylation efficiency and depression of uncoupled respiration in mitochondria under hypoxia. *Proc. Natl. Acad. Sci. USA* 97, 11080–11085.
- 10 Levenberg, S., Rouwkema, J., Macdonald, M., Garfein, E. S., Kohane, D. S., Darland, D. C., Marini, R., van Blitterswijk, C. A., Mulligan, R. C., d'Amore, P. A. and Langer, R. (2005) Engineering vascularised skeletal muscle tissue. *Nat. Biotechnol.* 23, 879–884.
- 11 Lussi, J. W., Falconnet, D., Hubbell, J. A., Textor, M. and Csucs, G. (2006) Pattern stability under cell culture conditions – A comparative study of patterning methods based on PLL-g-PEG background passivation. *Biomaterials* 27, 2534–2541.
- 12 Brown, R. A., Wiseman, M., Chuo, C. B., Cheema, U. and Nazhat, S. N. (2005) Ultrarapid engineering of biomimetic materials and tissues: Fabrication of nano- and microstructures by plastic compression. *Adv. Funct. Mater.* 15, 1762–1770.
- 13 Burt, A. and McGrouther, D. A. (1992) Production and use of skin cell cultures in therapeutic situation. In: *Animal Cell Biotechnology*, vol. 5, pp. 150–168, Spier, R. E., Griffiths, J. B. (eds.), Academic Press, New York.
- 14 Cheema, U., Yang, S. Y., Mudera, V., Goldspink, G. and Brown, R. (2003) 3D *in vitro* model of early skeletal muscle development. *Cell Motil. Cytoskeleton* 54, 226–236.
- 15 Cheema, U., Nazhat, S. N., Alp, B., Foroughi, F., Anandagoda, N., Mudera, V. and Brown, R. A. (2007) Fabricating tissues: Analysis of farming *versus* engineering strategies. *Biotechnol. Bioprocess. Eng.* 12, 9–14.
- 16 Seddon, B. M., Honess, D. J., Vojnovic, B., Tozer, G. M. and Workman, P. (2001) Measurement of tumor oxygenation: *In vivo* comparison of a luminescence fiber-optic sensor and a polarographic electrode in the p22 tumor. *Radiat. Res.* 155, 837–846.
- 17 Rong, Z., Cheema, U. and Vadgama, P. (2006) Needle enzyme electrode based glucose diffusive transport measurement in a collagen gel and validation of a simulation model. *Analyst* 131, 816–821.
- 18 Cooper, A. and Beasley, D. (1999) Hypoxia stimulates proliferation and interleukin-1 $\alpha$  production in human vascular smooth muscle cells. *Am. J. Physiol.* 277, H1326–H1337.
- 19 Falanga, V., Qian, S. W., Danielpour, D., Katz, M. H., Roberts, A. B. and Sporn, M. B. (1991) Hypoxia upregulates the synthesis of TGF-beta 1 by human dermal fibroblasts. *J. Invest. Dermatol.* 97, 634–637.
- 20 Kourembanas, S., Hannan, R. L. and Faller, D. V. (1990) Oxygen tension regulates the expression of the platelet-derived growth factor-B chain gene in human endothelial cells. *J. Clin. Invest.* 86, 670–674.
- 21 Steinbrech, D. S., Longaker, M. T., Mehrara, B. J., Saadeh, P. B., Chin, G. S., Gerrets, R. P., Chau, D. C., Rowe, N. M. and Gittes, G. K. (1999) Fibroblast response to hypoxia: The relationship between angiogenesis and matrix regulation. *J. Surg. Res.* 84, 127–133.
- 22 Ma, T., Yang, S.-T. and Kniss, D. A. (2001) Oxygen influences proliferation and differentiation in a tissue-engineered model of placental trophoblast-like cells. *Tissue Eng.* 7, 495–506.
- 23 Falanga, V. and Kirsner, R. S. (1993) Low oxygen stimulates proliferation of fibroblasts seeded as single cells. *J. Cell Physiol.* 154, 506–510.
- 24 Trentin, D., Hall, H., Wechsler, S. and Hubbell, J. A. (2006) Peptide-matrix-mediated gene transfer of an oxygen-insensitive hypoxia-inducible factor-1 alpha variant for local induction of angiogenesis. *Proc. Natl. Acad. Sci. USA* 103, 2506–2511.
- 25 Semenza, G. L. (1998) Hypoxia-inducible factor 1: master regulator of O<sub>2</sub> homeostasis. *Curr. Opin. Genet. Dev.* 8, 588–594.
- 26 Kumar, V. B., Kiran, M. S. and Sudhakaran, P. R. (2007) Endothelial cell response to lactate: Implication of PAR modification of VEGF. *J. Cell Physiol.* 211, 477–485.